DOI: 10.51790/2712-9942-2020-1-1-9

MATHEMATICAL MODEL AND SOFTWARE FOR AVALANCHE FORECASTING

Mikhail I. Zimin[1], **Olga A. Kumukova**[2], **Mikhail M. Zimin**[1]
[1] *2554620 ONTARIO LTD., Toronto, Canada, zimin7@yandex.ru*
[2] *High-Mountain Geophysical Institute, Nalchik, Russian Federation, kumukova@rambler.ru*

Abstract: the study presents mathematical models and software for avalanche forecasting. They take into account the avalanche occurrence rate for specific slopes. The database is also presented.

Keywords: snow, avalanche, forecasting, danger, mathematical models and software.

Cite this article: Zimin M. I., Kumukova O. A., Zimin M. M. Mathematical Model and Software for Avalanche Forecasting. *Russian Journal of Cybernetics*. 2020;1(1):63–80. DOI: 10.51790/2712-9942-2020-1-1-9.

МАТЕМАТИЧЕСКОЕ И ПРОГРАММНОЕ ОБЕСПЕЧЕНИЕ ДЛЯ ПРОГНОЗИРОВАНИЯ ВОЗМОЖНОСТИ СХОДА СНЕЖНЫХ ЛАВИН

М. И. Зимин[1], **О. А. Кумукова**[2], **М. М. Зимин**[1]
[1] *2554620 ONTARIO LTD., г. Торонто, Канада, zimin7@yandex.ru*
[2] *Высокогорный геофизический институт, г. Нальчик, Российская Федерация, kumukova@rambler.ru*

Аннотация: описано математическое и программное обеспечение для прогнозирования возможности схода снежных лавин. Учитываются данные о возникновении этих склоновых процессов с конкретных склонов. Описана база данных.

Ключевые слова: снег, лавина, прогноз, опасность, математическое и программное обеспечение.

Для цитирования: Зимин М. И., Кумукова О. А., Зимин М. М. Математическое и программное обеспечение для прогнозирования возможности схода снежных лавин. *Успехи кибернетики*. 2020;1(1):63–80. DOI: 10.51790/2712-9942-2020-1-1-9.

The paper is translated into English by the authors.

Introduction

RD 52.37.612-2000 Guideline [1] is currently used for avalanche danger forecasting in the Russian Federation. However, unexpected avalanches do occur, although rarely. Therefore, further improvement of the avalanche forecasting methods is of some interest.

The accuracy of avalanche forecasting can be improved by considering more extensive historical data. A separate database is created for each avalanche site. It complicates the forecasting center operations, but it certainly improves the quality of the risk estimation.

Avalanche Forecasting Algorithm

To simulate the local avalanche risk, we developed forecasting dependences. Their parameters were derived for the following conditions:

1. The number of unexpected avalanches does not exceed one in a thousand (in this case, a small slope process rarely results in human casualties, so the acceptable probability is relatively high.)
2. The number of correct forecasts should be as high as possible.

The forecasting dependence factors were estimated to the nearest hundredth.

The result was the following algorithm.

First, we check whether the avalanche danger is exceptionally high.

First, the following values are calculated [1, 2]:

$$p_{\alpha i} = [0.8\exp(-|\alpha - 35.0|/7.2)]^{3.1\{1+\exp[9(\alpha-90)]+\exp[9(14.0-\alpha)]\}}, \tag{1}$$

$$p_{li} = \begin{cases} [(1.65/\pi) arctg(L/16)]^{2.9\{1.0+\exp[2.2(7.1-L)]\}} \; at \; \alpha \le 58^\circ \\ [(1.54/\pi) arctg(L/2{,}6)]^{3.1\{1.0+\exp[142(0.12-L)]\}} \; at \; \alpha > 58^\circ \end{cases}, \tag{2}$$

$$p_{hi} = \left[\frac{1.71}{\pi} arctg\left(2.7h^{1.3}\right)\right]^{2.6\{1+\exp[3.6(51.0-100h)]\}}, \tag{3}$$

where $p_{\alpha i}$ accounts for the slope angle contribution to the exceptionally high avalanche danger occurrence; p_{li} accounts for the contribution of the avalanche nucleation zone length (hypotenuse) to the exceptionally high avalanche danger occurrence, p_{hi} accounts for the contribution of the slope snow layer thickness to the exceptionally high avalanche danger occurrence.

Then we estimate the comprehensive contribution of the slope angle, the avalanche nucleation area length (hypotenuse) and the slope snow layer thickness to the exceptionally high avalanche danger occurrence. For this purpose we estimated the parameters [1, 2]:

$$p_{\alpha i1} = p_{\alpha i}^{1-0.43p_{li}-0.47p_{hi}}, \tag{4}$$

$$p_{hi1} = p_{hi}^{1-0.49p_{\alpha i}-0.49p_{li}}, \tag{5}$$

$$p_{li1} = p_{li}^{1-0.13p_{\alpha i}-0.08p_{hi}}, \tag{6}$$

$$p_i = p_{\alpha i1} p_{li1} p_{hi1}, \tag{7}$$

where $\mathbf{p}_{\alpha i1}$ accounts for the slope angle contribution to the exceptionally high avalanche danger occurrence also taking into account the values of p_{hi} and $\mathbf{p}_{li}$; $\mathbf{p}_{hi1}$ accounts for the slope snow thickness contribution to the exceptionally high avalanche danger occurrence also taking into account the values of $\mathbf{p}_{\alpha i}$ and $\mathbf{p}_{li}$; $\mathbf{p}_{li1}$ accounts for the contribution of the avalanche nucleation area length (hypotenuse) to the exceptionally high avalanche danger occurrence taking into account the values of $\mathbf{p}_{\alpha i}$ and p_{hi}; p_i accounts for the comprehensive contribution of the slope angle, the avalanche nucleation area length (hypotenuse) and the slope snow layer thickness to the exceptionally high avalanche danger occurrence.

The following values are calculated [1, 2]:

$$p_{qi} = \left[\frac{2}{\pi} arctg(0.52q)\right]^{1-0.17p_i}, \tag{8}$$

$$d_{qi} = \begin{cases} 0.161\mathrm{q}\;, \text{ if } \mathrm{q} \le 46 \\ 2.8\mathrm{q} - 121.4\;, \text{ if } \mathrm{q} > 46, \end{cases} \tag{9}$$

where $p_{\alpha i}$ accounts for the total precipitation contribution to the exceptionally high avalanche danger occurrence; **q** is the total precipitation for the last day, $\mathbf{d}_{qi}$ accounts for the $\mathbf{p}_{qi}\mathbf{(q)}$ curve shape contribution to the exceptionally high avalanche danger occurrence.

$$p_{oi} = \left[\frac{1.97}{\pi} arctg\left(o^{0.63}\right)\right]^{1-0.15p_i}, \tag{10}$$

where $\mathbf{p}_{oi}$ accounts for the precipitation rate contribution to the exceptionally high avalanche danger occurrence; **o** is the average precipitation rate for the last 3 hours, mm/h

$$p_{vi} = \left[\frac{1.6}{\pi} arctg(0.8v)\right]^{1-0.2p_i}, \tag{11}$$

where $\mathbf{p}_{vi}$ accounts for the wind speed contribution to the exceptionally high avalanche danger occurrence, **v** is the wind speed, m/sec

$$p_{t10i} = \begin{cases} \left[\frac{2}{\pi} arctg(1.5g_{rt10})\right]^{1-0.05p_i} \; at \; \mathrm{t}_{10} \le -0.3 \\ \frac{2}{\pi} arctg[11.7(g_{rt10}+2.3)] \; at \; \mathrm{t}_{10} > -0.3 \end{cases}, \tag{12}$$

$$d_{t10i} = \begin{cases} 0.12g_{rt10}\, at\, t_{10} \leq -0.3 \\ 2.2(1.8 + g_{rt10})\, at > -0.3 \end{cases}, \tag{13}$$

$$g_{rt10} = \frac{|t_{10}|}{h_{10}}, \tag{14}$$

where $\mathbf{p}_{t10i}$ accounts for the 10-day average snow temperature gradient contribution to the exceptionally high avalanche danger occurrence; $\mathbf{g}_{rt10}$ is the 10-day average snow temperature gradient; $\mathbf{d}_{t10i}$ accounts for the $\mathbf{p}_{t10i}(\mathbf{t}_{10})$ curve shape contribution to the exceptionally high avalanche danger occurrence.

$$g_{rt10} = \frac{2|t|}{h + h_0}, \tag{15}$$

$\mathbf{g}_{rt10}$ is the average show layer temperature gradient for the entire snow-on-slope period, ^{o}C/m

$$p_{ti} = \begin{cases} \frac{2}{\pi} arctg(g_{rt} - 13.2)\, at\, t \leq -0.3 \\ \frac{2}{\pi} arctg(g_{rt} + 11.2)\, at\, t > -0{,}3 \end{cases}, \tag{16}$$

$$d_{ti} = \begin{cases} \frac{2}{\pi} arctg(0.06\tau)\, at\, t \leq -0.3 \\ \frac{2}{\pi} arctg\tau\ \ at\, t > -0.3 \end{cases}, \tag{17}$$

where $\mathbf{p}_{ti}$ accounts for the temperature gradient contribution to the exceptionally high avalanche danger occurrence; $\mathbf{d}_{ti}$ accounts for the $\mathbf{p}_u\mathbf{(t)}$ curve shape contribution to the exceptionally high avalanche danger occurrence.

The snow condition grade in terms of affecting the exceptionally high avalanche danger occurrence is [1, 2]:.

$$q_i = p_i^{1 - \frac{2}{\pi} arctg(0.4p_{oi} + d_{qi}p_{qi} + p_{vi} + d_{ti}p_{ti} + d_{t10i}p_{t10i})}. \tag{18}$$

If $q_i \geq 0.9$, we assume that an exceptionally high avalanche danger exists [1, 2]. Otherwise, we check whether we should expect a mass-scale, high-volume avalanching when from 10 to 50% of the avalanche catchment area is affected by the avalanche.

An “exceptionally high avalanche danger” forecast covers only the next day [1, 2]. Fort the next second and third days in this case the forecast is “unstable snow cover, large avalanches expected covering 10 to 50% of the avalanche catchment area” [1, 2].

A multi-step process is used to identify possible mass-scale, high-volume avalanching event.

First, the values [1, 2] are calculated:

$$p_{\alpha\, d} = p_{\alpha\, i}, \tag{19}$$

$$p_{l\, d} = p_{l\, i}, \tag{20}$$

$$p_{hd} = \left[\frac{1.71}{\pi} arctg(2.7h^{1,3})\right]^{2.6[1 + e^{3.2(38 - 100h)}]}, \tag{21}$$

where $p_{\alpha d}$ accounts for the slope angle contribution to the mass-scale, high-volume avalanching probability; p_{id} accounts for the contribution of the avalanche nucleation zone length (hypotenuse) to the mass-scale, high-volume avalanching probability; p_{hd} accounts for the contribution of the slope snow layer thickness to the mass-scale, high-volume avalanching probability.

Then we estimate the comprehensive contribution of the slope angle, the avalanche nucleation area length (hypotenuse) and the slope snow layer thickness to the mass-scale, high-volume avalanching probability. For this purpose we estimated the parameters [1, 2]:

$$p_{\alpha d1} = p_{\alpha d}^{1 - 0.43p_d - 0.47p_d}, \tag{22}$$

$$p_{hd1} = p_{hd}^{1 - 0.49p_{\alpha d} - 0.49p_{ld}}, \tag{23}$$

$$p_{li1} = p_{li}^{1-0.13p_{\alpha i}-0.08p_{hd}}, \quad (24)$$

$$p_d = p_{\alpha d1}p_{ld1}p_{hd1}, \quad (25)$$

where $\mathbf{p}_{\alpha d1}$ accounts for the slope angle contribution to the mass-scale, high-volume avalanching probability accounting for $\mathbf{p}_{hd}$ and $\mathbf{p}_{ld}$values; $\mathbf{p}_{hd1}$ accounts for the contribution of the slope snow layer thickness to the mass-scale, high-volume avalanching probability accounting for $\mathbf{p}_{\alpha d}$ and $\mathbf{p}_{ld}$values; $\mathbf{p}_{ld1}$accounts for the avalanche nucleation zone length (hypotenuse) to the mass-scale, high-volume avalanching probability accounting for $\mathbf{p}_{\alpha d}$ and $\mathbf{p}_{hd}$; $\mathbf{p}_d$accounts for the comprehensive contribution of the slope angle, the avalanche nucleation area length (hypotenuse) and the slope snow layer thickness to the mass-scale, high-volume avalanching probability.

The following values are calculated [1, 2]:

$$p_{qd} = \left[\frac{2}{\pi}arctg(0.8q)\right]^{1.0-0.9p_d}, \quad (26)$$

$$d_{qd} = \begin{cases} 0.71q, if\ q \le 10 \\ 1.65q - 15.79, if\ q > 10, \end{cases} \quad (27)$$

where $\mathbf{p}_{qd}$ accounts for the total precipitation contribution to the mass-scale, high-volume avalanching probability; $\mathbf{d}_{qd}$accounts for the $\mathbf{p}_{qd}\mathbf{(q)}$ curve shape contribution to the mass-scale, high-volume avalanching probability.

$$p_{od} = \left[(1{,}97/\pi)arctg\left(o^{1.3}\right)\right]^{1-0.05p_d}, \quad (28)$$

where $\mathbf{p}_{od}$ accounts for the last 3 h precipitation rate contribution to the mass-scale, high-volume avalanching probability

$$p_{vd} = [(1.4/\pi)arctgv]^{1-0.17p_d}, \quad (29)$$

where $\mathbf{p}_{vd}$ accounts for the wind speed contribution to the mass-scale, high-volume avalanching probability

$$d_{t10d} = \begin{cases} 0{,}62\mathrm{g}_{\mathrm{r\,t10}}\ at\ t_{10} \le -0{,}3\ 8\ \mathrm{g}_{\mathrm{r\,t10}} \le 13 \\ 1{,}26\mathrm{g}_{\mathrm{r\,t10}}\ at\ t_{10} \le -0{,}3\ 8\ \mathrm{g}_{\mathrm{r\,t10}} > 13 \\ 2{,}2(\mathrm{g}_{\mathrm{r\,t10}} + 1{,}8)\ at\ t_{10} > -0{,}3 \end{cases}, \quad (30)$$

$$p_{t10d} = \begin{cases} [(2.0/\pi)arctg(2.2g_{rt10})]^{1-0.17p_d}\ at\ t_{10} \le -0.3\ and\ \mathrm{g}_{\mathrm{r\,t10}} \le 13 \\ [(2.0/\pi)arctg(2.9g_{r\,t10})]^{1-0.22p_d}\ at\ t_{10} \le -0.3\ and\ \mathrm{g}_{\mathrm{r\,t10}} > 13 \\ (2.0/\pi)arctg[11.7(g_{r\,t10} + 2{,}3)]\ at\ t_{10} > -0.3 \end{cases}, \quad (31)$$

where $\mathbf{d}_{t10d}$ accounts for the $\mathbf{p}_{t10d}\mathbf{(g}_{rt10}\mathbf{)}$ curve shape contribution to the mass-scale, high-volume avalanching probability; $\mathbf{p}_{t10d}$ accounts for the 10-day average snow temperature gradient contribution to the mass-scale, high-volume avalanching probability

$$p_{t\,d} = \begin{cases} (2.0/\pi)arctg(g_{r\,t} - 9.2)\ at\ t \le -0.3 \\ (2.0/\pi)arctg(g_{r\,t} + 13.8)\ at\ t > -0.3 \end{cases}, \quad (32)$$

where $\mathbf{p}_{td}$ accounts for the contribution of the snow temperature gradient over the entire snow-on-slope period to the mass-scale, high-volume avalanching probability

$$p_{h0d} = \left[(1.95/\pi)arctg\left(h_0^{3,4}\right)\right]^{1-0.07p_d}, \quad (33)$$

where $\mathbf{p}_{h0d}$ accounts for the contribution of the initial show layer thickness to the mass-scale, high-volume avalanching probability

$$d_{td} = \begin{cases} (2{,}0/\pi)arctg(0{,}17\tau)\ at\ t \leq -0{,}3 \\ (2{,}0/\pi)arctg(2{,}44\tau)\ at\ t > -0{,}3 \end{cases}, \tag{34}$$

where $\mathbf{d}_{td}$ accounts for the contribution of the snow-on-slope period to the mass-scale, high-volume avalanching probability; τ is the snow-on-slope period.

The snow condition grade in terms of affecting the mass-scale, the high-volume avalanching probability is [1, 2]:

$$q_d = p_d^{\left[1-\frac{1.99}{\pi}arctg(0{,}4p_{od}+d_{qd}p_{qd}+p_{vd}+d_{td}p_{td}+0{,}7p_{h0d}+d_{t10d}p_{t10d})\right]}, \tag{35}$$

where $\mathbf{q}_d$ is the snow condition grade in terms of affecting the mass-scale, high-volume avalanching probability.

If $\mathbf{q}_d \geq 0.9$, then the forecast is “mass-scale, high-volume avalanching is expected covering 10 to 50% of the avalanche catchment area” [1, 2]. For the second day, the forecast is “unstable snow cover, large-scale avalanches expected covering 10 to 50% of the avalanche catchment area” [1, 2]. For the third day, the forecast is “unstable snow cover, small avalanching is expected covering up to 10% of the avalanche catchment area” [1, 2].

If $\mathbf{q}_d < 0.9$, we should check if the snow layer is unstable (avalanches are not guaranteed in this case.)

Possible snow cover instability is estimated as follows.

First, the values [1, 2] are calculated:

$$p_\alpha = p_{\alpha\, i}, \tag{36}$$

$$p_l = p_{l\, i}, \tag{37}$$

$$p_h = \left[(2/\pi)arctg(4.8h^{1.8})\right]^{2.3\,[1+3.2(22.0-100h)]}, \tag{38}$$

where p_α accounts for the slope angle contribution to the snow cover instability; p_i accounts for the contribution of the avalanche nucleation zone length (hypotenuse) to the snow cover instability; p_h accounts for the contribution of the slope length (hypotenuse) to the probability of snow cover instability.

Then we estimate the comprehensive contribution of the slope angle, the avalanche nucleation area length (hypotenuse) and the slope snow layer thickness to the probability of snow cover instability. For this purpose the values are calculated [1, 2]:

$$p_{\alpha 1} = p_\alpha^{1-0.43p_l-0.47p_h}, \tag{39}$$

$$p_{h1} = p_h^{1-0.49p_\alpha-0.49p_l}, \tag{40}$$

$$p_{l1} = p_l^{1-0.13p_\alpha-0.08p_h}, \tag{41}$$

$$p = p_{\alpha 1}p_{l1}p_{h1}, \tag{42}$$

where $\mathbf{p}_{\alpha 1}$accounts for the slope angle contribution to the probability of snow cover instability also taking into account the values of $_h$ and $\mathbf{p}_l$; p_{h1} accounts for the slope snow thickness contribution to the probability of snow cover instability also taking into account the values of $\mathbf{p}_\alpha$ and $\mathbf{p}_l$; $\mathbf{p}_{l1}$accounts for the contribution of the avalanche nucleation area length (hypotenuse) to the probability of snow cover instability taking into account the values of $\mathbf{p}_\alpha$ and $\mathbf{p}_h$; $\mathbf{p}$ accounts for the comprehensive contribution of the slope angle, the avalanche nucleation area length (hypotenuse) and the slope snow layer thickness to the probability of snow cover instability.

The following parameters are then determined:

$$p_q = \begin{cases} (2.0/\pi)arctg(0.12q)\ at\ q \leq 11 \\ [(2.0/\pi)arctg(q-10.968)]^{1-0.08p}\ at\ q > 11 \end{cases}, \tag{43}$$

$$d_q = \begin{cases} (2{,}0/\pi) actg(q/14{,}0) \; at \; q \le 11 \\ 14.6 \; at \; q > 11 \end{cases}, \tag{44}$$

where $\mathbf{p}_q$ accounts for the total precipitation contribution to the probability of snow cover instability; $\mathbf{d}_q$ accounts for the $\mathbf{p}_q\mathbf{(q)}$ curve shape contribution to the probability of snow cover instability.

$$p_o = \left[(1.97/\pi) arctg\left(o^{1.3}\right)\right]^{1-0.05p}, \tag{45}$$

where $\mathbf{p}_o$ accounts for the last 3 h precipitation rate contribution to the probability of snow cover instability

$$p_{vv} = [0.96 + 18.36(2.0/\pi)\operatorname{arctg}(1100 d_h)] \operatorname{arctg}[(v/3.2)^{1.7}], \tag{46}$$

$$p_v = 0.95^{1+e^{12(5.6-v)}} p_{vv}, \tag{47}$$

where $\mathbf{p}_v$ accounts for the contribution of the last day wind speed and snow layer thickness variation to the probability of snow cover instability; $\mathbf{d}_h$ is the snow layer thickness variation for the last day, m.

$$p_{h0} = \left[(1.95/\pi) arctg\left(h_0^{3.4}\right)\right]^{1-0.07p}, \tag{48}$$

where $\mathbf{p}_{h0}$ accounts for the contribution of the initial show layer thickness to the probability of snow cover instability

$$p_{t10} = \begin{cases} \{(1.98/\pi)\, arctg[4.2(g_{rt10} - 16.3)]\}^{1-0.11p} \; at \; t_{10} < -0.3 \; and \; g_{rt10} > 16.3 \\ 0.074(1.98/\pi)\, arctg[1.4(g_{rt10} - 16.3)] \; at \; t_{10} < -0.3 \; and \; g_{rt10} \le 16.3 \\ \{(2.0/\pi)\, arctg[4.8(g_{rt10} + 13)]\}^{1-0.08p} \; at \; t_{10} \ge -0.3 \end{cases}, \tag{49}$$

where $\mathbf{p}_{t10}$ accounts for the last 10 day-average temperature gradient contribution to the probability of snow cover instability

$$d_t = \begin{cases} 16.0\frac{2}{\pi} arctg(0.0017\tau) \; at \; t < -0.3 \; and \; g_{rt} > 9.6 \\ 0.9\frac{2}{\pi} arctg(0.0006\tau) \; at \; t < -0.3 \; and \; g_{rt} \le 9.6 \\ 9.0\frac{2}{\pi} arctg(\tau) \; at \; t \ge -0.3 \end{cases}, \tag{50}$$

where $\mathbf{d}_t$ accounts for the contribution of the initial snow-on-slope period to the probability of snow cover instability

$$p_t = \begin{cases} \frac{2}{\pi}\{arctg[4.6(g_{rt} - 8.6)]\}^{1.0-0.05p}, \; if \; g_{rt} > 9.6 \; and \; t < -0.3 \\ \frac{0.17}{\pi} arctg[1.1(g_{rt} - 9.6)], \; if \; g_{rt} \le 9.6 \; and \; t < -0.3 \\ \frac{2}{\pi} arctg[3.8(g_{rt} + 6.0)], \; if \; t \ge -0.3 \end{cases}, \tag{51}$$

where $\mathbf{p}_t$ accounts for the contribution of the snow temperature gradient to the probability of snow cover instability [1, 2].

The snow condition grade in terms of affecting the probability of snow cover instability is

$$q_p = p^{1-\frac{2}{\pi} arctg(0{,}4p_o + d_q p_q + p_v + d_t p_t + 0.7p_{ho} + 12.3p_{t10})}. \tag{52}$$

where $\mathbf{q}_d$ is the snow condition grade in terms of affecting the probability of snow cover instability.

Then the avalanche danger is evaluated based on the experimental data. Pattern recognition methods are used. The basic training sample is:

6 49
1 1 26.0 0.9 16.3 0.5 120.0 11.0
2 0 11.0 0.3 2.9 0.5 70.0 0.0
3 1 15.0 0.4 0.3 0.0 32.0 1.0
4 1 16.0 0.5 1.0 0.2 96.0 2.0
5 0 10.0 0.2 2.3 0.4 40.0 0.0
6 0 38.0 2.0 14.1 0.1 90.0 10.0
7 1 42.0 2.2 1.8 1.1 101.0 7.0
8 0 9.0 0.3 2.0 0.4 54.0 1.0
9 0 13.0 0.2 0.0 0.0 120.0 0.0
10 1 42.0 1.8 7.9 0.6 37.0 12.0
11 1 35.0 1.8 7.3 0.8 54.0 3.0
12 0 13.0 0.2 0.9 0.1 80.0 1.0
13 1 14.0 0.3 1.1 0.0 25.0 2.0
14 0 14.0 0.4 2.9 0.6 160.0 1.0
15 1 38.0 0.2 1.3 0.2 80.0 5.0
16 1 14.0 0.3 0.7 0.0 50.0 0.0
17 0 10.0 0.2 0.8 0.0 130.0 0.0
18 1 25.0 1.5 9.3 1.9 80.0 8.0
19 1 17.0 0.3 0.6 0.0 85.0 1.0
20 0 11.0 0.1 0.7 0.0 120.0 1.0
21 1 32.0 1.4 24.1 0.2 70.0 4.0
22 0 11.0 0.3 2.9 0.5 40.0 0.0
23 1 14.0 0.3 2.1 0.3 70.0 0.0
24 0 19.0 0.3 2.3 0.5 65.0 1.0
25 1 42.0 1.7 14.3 1.5 115.0 9.0
26 1 15.0 0.4 0.8 0.0 50.0 0.0
27 0 11.0 0.1 2.8 0.0 57.0 1.0
28 1 38.0 2.1 16.5 1.6 76.0 5.0
29 0 10.0 0.2 1.4 0.0 25.0 2.0
30 0 17.0 0.2 1.1 0.3 130.0 0.0
31 0 19.0 0.1 0.0 0.0 133.0 3.0
32 1 40.0 2.1 8.1 0.2 70.0 11.0
33 0 11.0 0.1 1.0 0.0 130.0 0.0
34 1 14.0 0.3 1.0 0.0 90.0 1.0
35 0 17.0 0.3 0.2 0.0 150.0 1.0
36 1 53.0 1.3 7.4 0.6 137.0 1.0
37 1 15.0 0.2 2.8 0.2 23.0 2.0
38 0 12.0 0.3 0.4 0.0 60.0 12.0
39 0 9.0 0.3 2.6 0.6 30.0 1.0
40 0 15.0 0.2 2.9 0.0 60.0 0.0
41 1 31.0 2.2 19.5 0.0 87.0 14.0
42 0 9.0 0.2 2.0 0.5 29.0 0.0
43 0 42.0 2.1 6.4 0.6 115.0 13.0
44 1 26.0 2.0 4.4 0.4 86.0 4.0
45 1 14.0 0.3 2.9 0.6 58.0 1.0
46 0 11.0 0.1 0.0 0.0 95.0 2.0
47 0 40.0 2.0 13.4 0.1 98.0 9.0
48 0 11.0 0.3 0.4 0.0 63.0 0.0
49 1 36.0 2.2 10.2 1.2 49.0 6.0

The first line contains the number of points and the number of variables. Each subsequent line contains point number, the situation code (0: no avalanche, 1: avalanche), slope angle (degrees), slope snow thickness (m), total precipitation over the last 24 h (mm), precipitation rate over the last 3 h (mm/h), slope length (hypotenuse), (m), wind speed (m/s.)

The sample can be supplemented with experimental data for a specific area.

Two pattern recognition algorithms were used [3]. In the first one, the separating surface passes through the midpoint of the line connecting the centers of scattering perpendicular to it. The second select selects the closest point.

$\mathbf{p}_a$ values are estimated to reduce the fuzziness:

$$p_a = q_p^{\frac{1+1.05u_1+1.05u_2}{1+1.05w_1+1.05w_2}}, \tag{53}$$

and

$$p_a^* = p_a^{(1-p_a)/1.1}. \tag{54}$$

When the first algorithm identifies avalanche danger, then $\mathbf{u}_1 = 0$ and $\mathbf{w}_1 = 0.5$. When the first algorithm identifies no avalanche danger, then $\mathbf{u}_1 = 0.5$ and $\mathbf{w}_1 = 0$; when the second algorithm identifies avalanche danger, then $\mathbf{u}_2 = 0$ and $\mathbf{w}_2 = 0.5$, when the second algorithm identifies no avalanche danger, then $\mathbf{u}_2 = 0.5$ and $\mathbf{w}_2 = 0$.

If $\mathbf{p}_a \geq 0.32$, then the snow is unstable. Otherwise, there is no avalanche danger.

If $\mathbf{p}_a \geq 0.32$ and $\mathbf{p}^*{}_a < 0.9$, the next day forecast is “unstable snow cover, small avalanching is expected covering up to 10% of the avalanche catchment area”. If $\mathbf{p}_a \geq 0.32$ and $\mathbf{p}^*{}_a \geq 0.9$, the next day forecast should be “unstable snow cover, large-scale avalanching is expected covering 10to 50% of the avalanche catchment area”, and for the second day the forecast should be “unstable snow cover, small avalanching is expected covering up to 10% of the avalanche catchment area”.

If the day-average temperature exceeds 0.4 ^{o}C, and the snow thickness exceeds 0.52 m, i.e. $65^o \geq \alpha > 15^o$ and $\mathbf{l} > 60$ m, the next day forecast is “unstable snow cover, large-scale avalanches expected covering 10 to 50% of the avalanche catchment area”. For the second day, the forecast is “unstable snow cover, small avalanching is expected covering up to 10% of the avalanche catchment area”.

If the day-average temperature exceeds -0.2 ^{o}C, 0.52 m $\geq \mathbf{h} >$0.22 m, $65^o \geq \alpha > 15^o$ and $\mathbf{l} > 6$ m, the next day forecast is “unstable snow cover, small avalanches expected covering up to 10% of the avalanche catchment area”.

The snow layer thickness used shall be reduced by the thickness of the top layer with its snow density exceeding 430 kg/m^3.

The seismic load is accounted as follows [2]. As the simulation shows, the avalanche danger during an earthquake does not change, if we use the following values instead of $\mathbf{h}$ and $\mathbf{q}$:

$$h_s = k_s \left[h - (1 - p_{eI} k_\rho k_e) h_{430} \right], \tag{55}$$

$$q_s = q + p_{eI} q_e, \tag{56}$$

where $\mathbf{h}_{430}$ is the snow layer thickness starting at the Earth surface with its density exceeding 430 kg/m^3, $\mathbf{p}_{eI}$ is the probability of I points (MSK-81 scale) earthquake

$$k_\rho = \frac{2}{\pi} arctg \left\{ 0.0000149 \cdot \left[I \cdot \left(\frac{910}{\rho_{430}} \right) \right]^{6.906} \right\}, \tag{57}$$

$$k_e = \frac{2}{\pi} arctg(3.972 \cdot 10^{-9} \cdot I^{9.438}), \tag{58}$$

$$k_s = \left\{ \begin{array}{c} 1 \; at \, I < 5 \\ 1 + 0.2 p_{eI}(I - 5) \; at \, 5 \leq I < 8 \\ 1 + 0{,}32 p_{eI}(I - 5) \; at \, I \geq 8 \end{array} \right., \tag{59}$$

$$q_e = \begin{cases} 0\,at\,I < 5 \\ 4.4(I-5)\,at\,5 \le I < 8 \\ 16.2(I-5)\,at\,I \ge 8 \end{cases}, \tag{60}$$

where **I** is the earthquake intensity at the Earth surface (MSK-81 scale), ρ_{430} is the average density of the snow layer starting at the Earth surface with its density > 430 kg/m^3.

To further refine the avalanche forecasting, historical data are also used. Snow thickness, total precipitation, precipitation intensity, wind speed (max gust) and air temperature for the last 24 hours are considered. Since the presence of slope snow is required for an avalanche, similar to the almost significant confidence probability [4], the current value is matched against the past value of 0.95. For the other parameters, a value of 0.9 is used. It corresponds to a confidence level value of 0.9, which is feasible in real life [5].

A decision whether a particular situation is similar to one of the avalanche dangers that occurred in the past is based on the balance of probabilities standard [6]. It means that the fact is proved if, with the evidence presented, it can be concluded that the fact rather occurred than not. Therefore, to identify the slope snow condition as similar to one of the past avalanche dangers, the snow thickness and any other two parameters are required to match it.

Table 1

Avalanche Danger in the Trans-Kam Area in November 1998

Date	τ,h	q,mm	o,mm/h	v,m/s	$q_f$mm	h[m]	t_{24}[^{o}C]	Avalanching
10.111998	24	3	0	1	0	0.03	-6.0	-
11.111998	48	0.4	0	4	0	0.07	-6.0	-
12.111998	72	0	0	2	0	0.05	-3.1	-
13.111998	0	0	0	2	0	0.03	0.4	-
14.111998					0	0	3.6	-
15.111998					0	0	3.2	-
16.111998					0	0	2.4	-
17.111998					0	0	2.1	-
18.111998	24	21.8	1	1	0	0.01	2.1	-
19.111998	48	14.2	2	2	0	0.02	1.1	-
20.111998					0	0	-0.3	-
21.111998					0	0	-0.1	-
22.111998					0	0	0.3	-
23.111998					0	0	-0.5	-
24.111998					0	0	-1.1	-
25.111998					0	0	-0.2	-
26.111998					0	0	3.3	-
27.111998					0	0	1.4	-
28.111998	24	12.1	0	2	0	0.02	0.1	-
29.111998	48	0	0	3	0	0.02	-0.3	-
30.111998	72	25.5	0	1	20.0	0.26	-0.5	-

An individual database shall be compiled for each avalanche catchment area. Excel was used for this purpose. The software can connect to code written, for example, in C++. In this way, the computation routine and the data storage system are combined, to take full advantage of both C++ Builder and Excel. Moreover, Excel is quite effective for creating simple databases and has a range of data visualization tools. Finally, it is easy to use. The general avalanche danger forecasting method can be further adapted to specific conditions. In some cases, the forecasting can be significantly refined, because it considers various local features not taken into account in the generic algorithm. Some abnormal cases which sometimes occur in highly unusual circumstances are also considered.

Avalanche Danger Trend Forecasting Algorithm

The snow instability grade, mass-scale, large-volume avalanching, or exceptionally high avalanche danger situations may change in time. As the equations show, any of these functions can asymptotically tend to one, asymptotically tend to zero, be constant, or oscillate. Accordingly, special functions are required to approximate their time dependences.

We should also note that it is possible to obtain only a very limited raw data sample, so the dependency generation method should match the amount of data and the complexity of the resulting function.

In this case, the most appropriate one is the structural risk minimization method providing such a capability. Besides, [7] describes the use of complex functions in this method as required for estimating the avalanche danger trend.

Avalanche danger often remains unchanged for a long time. For example, the “no avalanche danger” situation persisted in the Trans-Kam region in November 1998 for three weeks, as shown in Table 1. In the table, $\mathbf{q}_f$ is the expected total precipitation for the next day.

Another example is an almost constant avalanche risk level ”unstable snow cover, small avalanching is expected covering up to 10% of the avalanche catchment area” in January 1999. The data are shown in Table 2.

Table 2

Avalanche Danger in the Trans-Cam Area in January 1999

Date	τ, h	q, mm	o, mm/h	v, m/s	q_f mm	h [m]	t_{24} [°C]	Forecast for this day	Avalanching
01.01 1999	840	0.8	0.27	3	0	0.50	-15.3	Unstable snow cover, small avalanching is expected covering up to 10% of the avalanche catchment area (as of 31.12.1998)	-
02.01 1999	864	0	0	1	0	0.45	-9.7	Unstable snow cover. Large avalanching is expected covering from 10% to 50% of the avalanche catchment area (as of 01.01.1999)	-
03.01 1999	888	0	0	3	0	0.40	-7.5	Unstable snow cover, small avalanching is expected covering up to 10% of the avalanche catchment area (as of 02.01.1999)	-
04.01 1999	912	0	0	1	0	0.40	-5.6	Unstable snow cover, small avalanching is expected covering up to 10% of the avalanche catchment area (as of 03.01.1999)	-
05.01 1999	936	0	0	1	0	0.40	-3.4	Unstable snow cover, small avalanching is expected covering up to 10% of the avalanche catchment area (as of 04.01.1999)	Mass avalanching from the point.
06.01 1999	960	0	0	1	0	0.39	-5.2	Unstable snow cover, small avalanching is expected covering up to 10% of the avalanche catchment area (as of 05.01.1999)	Mass avalanching from the point
07.01 1999	984	0	0	1	0	0.38	-7.1	Unstable snow cover, small avalanching is expected covering up to 10% of the avalanche catchment area (as of 06.01.1999)	50 m^3 snow lenticle Stopped in the transit zone

Date	τ, h	q, mm	o, mm/h	v, m/s	q_f mm	h [m]	t_{24} [°C]	Forecast for this day	Avalanching
08.01 1999	1008	0	0	2	0	0.38	-5.4	Unstable snow cover, small avalanching is expected covering up to 10% of the avalanche catchment area (as of 07.01.1999)	100 m^3 snow lenticle, catchment area No. 91 Mass avalanching from the point
09.01 1999	1032	0	0	1	0	0.37	-4.9	Unstable snow cover, small avalanching is expected covering up to 10% of the avalanche catchment area (as of 08.01.1999)	-
10.01 1999	1056	0	0	3	7.0	0.37	-4.6	Unstable snow cover, small avalanching is expected covering up to 10% of the avalanche catchment area (as of 09.01.1999)	-
11.01 1999	1080	3.2	0.36	2	0	0.42	-2.4	Unstable snow cover, small avalanching is expected covering up to 10% of the avalanche catchment area (as of 10.01.1999)	Mass avalanching from the point
12.01 1999	1104	0	0	3	0	0.40	-8.9	Unstable snow cover, small avalanching is expected covering up to 10% of the avalanche catchment area (as of 11.01.1999)	Mass avalanching from the point
13.01 1999	1128	0	0	1	0	0.40	-6.6	Unstable snow cover, small avalanching is expected covering up to 10% of the avalanche catchment area (as of 12.01.1999)	-
14.01 1999	1152	0	0	2	0	0.38	-4.9	Unstable snow cover, small avalanching is expected covering up to 10% of the avalanche catchment area (as of 13.01.1999)	-
15.01 1999	1176	0	0	1	0	0.38	-3.7	Unstable snow cover, small avalanching is expected covering up to 10% of the avalanche catchment area (as of 14.01.1999)	-
16.01 1999	1200	0	0	2	0	0.38	-5.2	Unstable snow cover, small avalanching is expected covering up to 10% of the avalanche catchment area (as of 15.01.1999)	-
17.01 1999	1224	0	0	1	0	0.37	-4.8	Unstable snow cover, small avalanching is expected covering up to 10% of the avalanche catchment area (as of 16.01.1999)	-
18.01 1999	1248	0	0	2	0	0.35	-4.9	Unstable snow cover, small avalanching is expected covering up to 10% of the avalanche catchment area (as of 17.01.1999)	-
19.01 1999	1272	0	0	3	0	0.35	-5.2	Unstable snow cover, small avalanching is expected covering up to 10% of the avalanche catchment area (as of 18.01.1999)	-

Date	τ, h	q, mm	o, mm/h	v, m/s	q_f mm	h [m]	t_{24} [^oC]	Forecast for this day	Avalanching
20.01 1999	1296	0	0	2	1	0.34	-5.9	Unstable snow cover, small avalanching is expected covering up to 10% of the avalanche catchment area (as of 19.01.1999)	-
21.01 1999	1320	0	0	2	0	0.34	-6.0	Unstable snow cover, small avalanching is expected covering up to 10% of the avalanche catchment area (as of 20.01.1999)	-
22.01 1999	1344	0	0	3	0	0.34	-6.1	Unstable snow cover, small avalanching is expected covering up to 10% of the avalanche catchment area (as of 21.01.1999)	-
23.01 1999	1368	0	0	3	0	0.34	-6.1	Unstable snow cover, small avalanching is expected covering up to 10% of the avalanche catchment area (as of 22.01.1999)	-
24.01 1999	1392	0	0	2	1	0.33	-8.7	Unstable snow cover, small avalanching is expected covering up to 10% of the avalanche catchment area (as of 23.01.1999)	-
25.01 1999	1416	0	0	2	0	0.33	-8.7	Unstable snow cover, small avalanching is expected covering up to 10% of the avalanche catchment area (as of 24.01.1999)	Two shells were fired. One avalanche was triggered
26.01 1999	1440	0	0	2	0	0.33	-9.4	Unstable snow cover, small avalanching is expected covering up to 10% of the avalanche catchment area (as of 25.01.1999)	-
27.01 1999	1464	0	0	4	0	0.33	-4.9	Unstable snow cover, small avalanching is expected covering up to 10% of the avalanche catchment area (as of 26.01.1999)	-
28.01 1999	1488	0	0	3	0	0.33	-8.4	Unstable snow cover, small avalanching is expected covering up to 10% of the avalanche catchment area (as of 27.01.1999)	-
29.01 1999	1512	0	0	3	0	0.33	-6.9	Unstable snow cover, small avalanching is expected covering up to 10% of the avalanche catchment area (as of 28.01.1999)	-

The fact that the snow was unstable is confirmed by the avalanches on 5.01-8.01, 11.01-12.01 and the slope process initiation after the shelling of the avalanche catchment area on 25.01.

The risk of avalanches can increase quickly and then decrease. This is shown in Table 3.

Table 3

Avalanche danger in the Trans-Cam area in February 1999

Date	τ, h	q, mm	o, mm/h	v, m/s	q_f mm	h [m]	t_{24} [^oC]	Forecast for this day	Avalanching
16.02 1999	1944	2.3	2.3	4	2	0.57	-2.2	Unstable snow cover, small avalanching is expected covering up to 10% of the avalanche catchment area (as of 15.02.1999)	-

Date	τ, h	q, mm	o, mm/h	v, m/s	q_f mm	h [m]	t_{24} [^oC]	Forecast for this day	Avalanching
17.02 1999	1968	12.3	0.83	4	15	0.67	-3.6	Unstable snow cover, small avalanching is expected covering up to 10% of the avalanche catchment area (as of 16.02.1999)	-
18.02 1999	1992	29.4	1.0	2	1	0.89	-2.6	Avalanche danger. Large avalanching is expected covering 10 to 50% of the avalanche catchment area (as of 17.02.1999). The forecast is simulated	Catchment areas (CA) 43, 49, 75[a], 83, 87, 91' generated 100 m^3 avalanches; AA 41, 55, 56, 57, 80, 82, 93, 50, 39, 40, 60, 69, 71, 84, 88: 200 m^3; CA 65, 81: 300 m^3; CA 28, 46: 500 m^3; CA 37, 72, 73, 74,91: 1,000 m^3; CA 102, 103: 2,000 m^3; CA 35, 67, 70: 5,000 m^3; CA74[a]: 50,000 m^3
19.02 1999	2016	5.5	1.4	4	30	0.64	-4.3	Unstable snow cover. Large avalanching is expected covering 10% to 50% of the avalanche catchment area (as of 17.02.1999)	CA 205[a] generated 15,000 m^3 avalanches; CA No. 3: 5,000 m^3, CA No. 5: 200 m^3, CA No. 4: 100 m^3. 8 shells were fired, 8 avalanches triggered
20.02 1999	2040	31.7	1.32	8	2	1.27	-5.7	Unstable snow cover. Large avalanching is expected covering 10% to 50% of the avalanche catchment area (as of 19.02.1999)	CA No. 91 generated an avalanche exceeding 1,000 m^3. The avalanche blocked the river and the road
21.02 1999	2064	0	0	4	2	1.15	-11.2	Avalanche danger. Large avalanching is expected covering 10 to 50% of the avalanche catchment area (as of 20.02.1999)	Twelve shells were fired. Six avalanches were triggered
22.02 1999	2088	0	0	2	0	1.05	-7.2	Unstable snow cover. Large avalanching is expected covering 10% to 50% of the avalanche catchment area (as of 20.02.1999)	-
23.02 1999	2112	0	0	1	0	0.92	-4.4	Unstable snow cover, small avalanching is expected covering up to 10% of the avalanche catchment area (as of 20.02.1999)	CA No. 74[a] generated a 2,000 m^3 avalanche; CA No. 103: 500 m^3; CA No. 102: 200 m^3

Date	τ, h	q, mm	o, mm/h	v, m/s	q_f mm	h [m]	t_{24} [^oC]	Forecast for this day	Avalanching
24.02 1999	2136	0	0	2	8	0.95	-2.1	Unstable snow cover, small avalanching is expected covering from 10% to 50% of the avalanche catchment area (as of 23.02.1999)	-
25.02 1999	2160	0.13	0.13	2	0	0.94	-3.0	Unstable snow cover, small avalanching is expected covering from 10% to 50% of the avalanche catchment area (as of 24.02.1999)	- -
26.02 1999	2184	0.3	0.3	2	3	0.94	-7.6	Unstable snow cover, small avalanching is expected covering up to 10% of the avalanche catchment area (as of 25.02.1999)	- -

On 18.02 and 21.02 there was a sharp avalanche danger increase which quickly decreased. The forecasting is confirmed by both the mass avalanches and a successful avalanche triggering.

In particular, the Chebyshev polynomials can be used to describe a constant, increasing, and first increasing, then decreasing avalanche danger. This is particularly efficient when we should determine whether the risk of avalanches remains constant.

The Chebyshev polynomials are as follows [8]:

$$Q_0 = 1, \tag{61}$$

$$Q_1 = x, \tag{62}$$

$$Q_2 = 2x^2 - 1, \tag{63}$$

$$Q_3 = 4x^3 - 3x. \tag{64}$$

The application of complex functions to the structural risk minimization method is presented in [9]. First, the values of $\mathbf{z}_i = \mathbf{f}(\mathbf{x}_i)$ are estimated, and then $\mathbf{y}(\mathbf{z})$ relation is fitted. We can reasonably choose a special function to describe the avalanche danger trend.

The snow condition grade in terms of affecting the avalanche danger occurrence can also increase or decrease asymptotically. The following functions are suitable for describing the dependencies

$$y(x) = \frac{2}{\pi} arctg(ax), \tag{65}$$

where **a** is an unknown coefficient

$$y(x) = th(ax). \tag{66}$$

To describe an oscillatory process we can use a function as follows

$$y(x) = \sin(ax + b), \tag{67}$$

where **a, b** are unknown coefficients.

As an example, we can analyze the trend of snow condition grade in terms of affecting the exceptionally high avalanche danger occurrence from the initial data listed in Table 4. The plot is shown in Fig. 1.

The estimations showed that it is best approximated by function (66). The fitted relation is $\mathbf{q_1(t) = 0.309t + 0.299th(t/15)}$. Its limit value is less than 0.9, so reaching the exceptionally high avalanche danger is not expected.

Avalanche Danger Forecasting Software

The **asf-3** software can be used to assess avalanche danger. Its initial window is shown in Fig. 2.

Table 4

Exceptionally high avalanche danger occurrence vs. time (t: time)

t, hours	0	3	6	9	12	15	18	21	24	27	30	33
$\mathbf{q}_i$	0.322	0.356	0.397	0.445	0.501	0.534	0.562	0.573	0.584	0.595	0.602	0.607

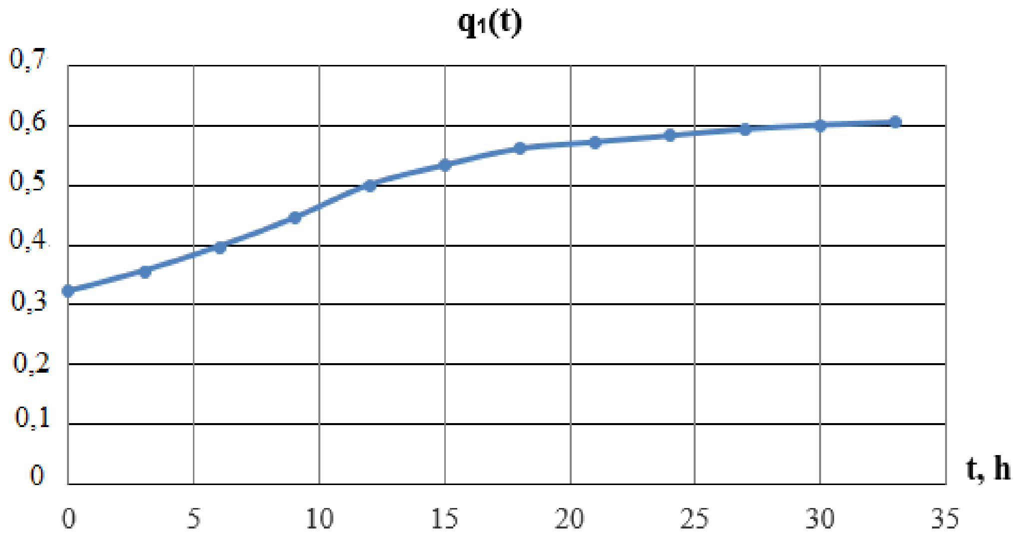

Figure 1. *Initial dependence for the exceptionally high avalanche danger occurrence*

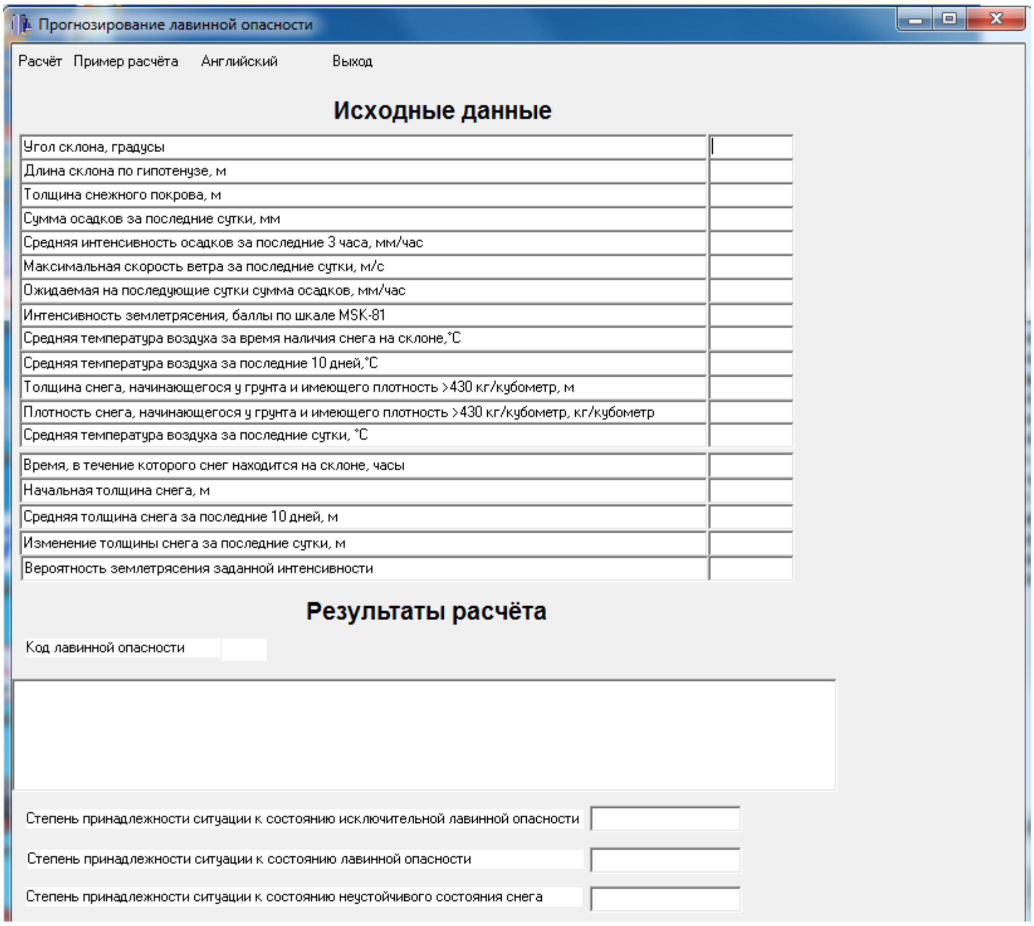

Figure 2. *The asf-3 software initial window*

The software can not only assess the current situation, but assess unstable snow grade, avalanche danger, and exceptionally high avalanche danger occurrence at different points in time.

To estimate the optimal complex function coefficients, it is generally required to solve a system of transcendental equations. A modified method described in [2] is used for this purpose. Let us define the function $\mathbf{F}(\mathbf{x}_1, \mathbf{x}_2, \ldots, \mathbf{x}_n)$. First, random coordinate values are selected: $\mathbf{x}_1 = \mathbf{x}_{11}$, $\mathbf{x}_2 = \mathbf{x}_{21}$, $\ldots$, $\mathbf{x}_n = \mathbf{x}_{n1}$. Then the values $\mathbf{x}_2$, $\mathbf{x}_3, \ldots$, $\mathbf{x}_n$ are fixed, while $\mathbf{x}_1$ is changed randomly. After that, the target function vs. $\mathbf{x}_1$ relation is found in the specified one-dimensional section with the structural risk minimization method [10, 11] using a class of Chebyshev polynomials [8]. Then its extremum is identified and the variable value is fixed. After that, in contrast to the algorithm described in [2], near the point of extremum an interval is defined. Its start and end points are estimated as

$$x_{1N} = x_{1\,\min} + 0.62(x_{1E1} - x_{1\,\min}), \tag{68}$$

$$x_{2N} = x_{1E1} + 0.38(x_{1\,\max} - x_{1E1}), \tag{69}$$

where $\mathbf{x}_{1E1}$ is the $\mathbf{x}_1$ coordinate of the found extremum point, $\mathbf{x}_{1min}$ is the start point of the $\mathbf{x}_1$ range; $\mathbf{x}_{1max}$ is the end point of the $\mathbf{x}_1$ range, $\mathbf{x}_{1N}$ is the new start point of the $\mathbf{x}_1$ range; $\mathbf{x}_{2N}$ is the new end point of the $\mathbf{x}_1$ range. It is the golden ratio extensively used in various fields [7]. Then the extremum search is repeated in a new interval, and the value of $\mathbf{x}_1$ at the new point is fixed.

The procedure is then applied to all the variables using the previously found optimal values of the preceding variables. The more starting points, the less chance of missing the global extremum [4].

The choice of a structural risk minimization method is governed by the following. Solving the system of transcendental equations is rather time-consuming, so the number of experimental points in one-dimensional sections is limited. Besides, as the initial data are fuzzy, the solutions contain some interference. The problems with developing dependencies from small samples are quite different from the classical problems of reconstructing dependencies from large samples. The difference is that for a limited sample size it is required to balance the dependence complexity with the amount of available empirical data.

It is advisable to apply the structural risk minimization method [10, 11]. Its essence is as follows. If we define a structure within an admissible set of solutions, i.e., a system of nested sets, each of them containing more and more complex solutions, then along with empirical risk minimization for its elements there is an opportunity to optimize the estimation quality by structure elements. This makes it possible to find a solution that gives a better guaranteed average risk minimum compared to a solution that produces an empirical risk minimum across the entire admissible set.

The structural risk minimization method applications for a given amount of information enables us to find the optimal number of members of the series that approximates the dependence. An arbitrary choice of this parameter can lead to a paradox. Suppose we need to reconstruct the dependence $\mathbf{y=f(x)}$ from ten experimental points. In this case, the empirical risk is zero when using the 9th-degree polynomial. However, the optimal degree of polynomial $\mathbf{n}$ can be 1.

With the structural risk minimization method, the regression fitting problem is reduced to minimizing the following value [10]:

$$J(k) = I_E(k)\Omega, \tag{70}$$

where $\mathbf{J(k)}$ is the average risk, $\mathbf{I}_e\mathbf{(k)}$ is the empirical risk, $\mathbf{k}$ identifies a particular function of a certain class, Ω is a variable.

As the sample volume increases, the Ω value always tends to one [10], although it differs in each specific case, if the sample is small, it may deviate significantly from 1. Then a function that produces a small empirical risk may not yield a small average risk.

There are different classes of basis functions. Chebyshev polynomials are easy to compute and enable to solve a wide range of dependence reconstruction problems. Besides, their use minimizes the max error. It is important when there are large errors in the raw data.

Then $\mathbf{y(x)}$ is presented as a series

$$y(x) = \sum_{i=0}^{k} \alpha_i Q_i(x), \tag{71}$$

where α_i is the $\mathbf{i}$th expansion factor, $\mathbf{Q}_i$ $\mathbf{(x)}$ is a Chebyshev polynomial of the $\mathbf{i}$th power.

With such a representation, the empirical risk functional is [10]:

$$I_E = \frac{1}{l}\sum_{j=1}^{l}\left[y_j - \sum_{i=0}^{k}\alpha_i Q_i(x_j)\right]^2, \tag{72}$$

where ℓ is the sample volume.

At a fixed maximum polynomial degree, the αi coefficients when the empirical risk is at its minimum are calculated by solving a system of linear algebraic equations [10]:

$$\Phi^T\Phi[\alpha] = \Phi^T[y]^T, \tag{73}$$

where Φ is a matrix of Chebyshev polynomial values at the points of interest, **[y]** is a row matrix of the **y** values at the points of interest, **[**α**]** is a column matrix of the α_i factors.

The estimated approximation quality valid for any random sample with the probability **1-**η is expressed as [10]:

$$J(k) = \frac{I_M}{1 - \sqrt{\frac{(k+1)\left[\ln\left(\frac{l}{k+1}\right)+1\right]-\ln\eta}{l}}}, \tag{74}$$

where **1-**η is the probability of the estimate (2.2.11) being valid, **J(k)** is the average risk.

(74) depends on the degree of the polynomial **k**. The degree at which **J(k)** is the smallest is the optimal degree of polynomial approximation. The regression function itself is approximated by a polynomial of this degree

minimizing the empirical risk functional.

Since Chebyshev polynomials are orthogonal on the interval **[-1, 1]**, if the independent variable values are not specified within this range, they shall be reduced to it as follows [10]:,

$$x_i = \frac{(x_{gi} - c_1)}{c_2},$$

where $\mathbf{x}_i$ is the independent variable values reduced to [-1, 1], $\mathbf{x}_{gi}$ are the initial independent variable values

$$c_1 = \frac{(x_{g\max} + x_{g\min})}{2},$$

$$c_2 = \frac{(x_{g\max} - x_{g\min})}{2},$$

where $\mathbf{x}_{gmin}$ is the min independent variable value, $\mathbf{x}_{gmax}$ is the max independent variable value.

It is possible to implement the algorithm with Excel. In the same system, one can create databases and plot graphs. It should be noted C++ programs can connect to Excel files.

Conclusion

The mathematical model and software for avalanche forecasting based on RD 52.37.612-2000 Guidelines, historical avalanche databases, and avalanche danger trend evaluation ensure acceptable safety in avalanche-affected areas. They can be used for the planning and implementation of various preventive measures.

REFERENCES

1. Zimin M. I. *Avalanche Forecasting*. St. Petersburg: Gidrometeoizdat; 2000. 16 p. (In Russ.)
2. Eskov V. M., Gavrilenko T. V., Zimin M. I., Zimina S. A. *Neural Network-Based Identification and Studying Chaotic Dynamics Systems*. Tula: Izdatel'stvo TuLGU; 2016. 398 p. (In Russ.)
3. Kuzin L. T. *Fundamentals of Cybernetics.* V. 2. M.: Ehnergiya; 1979. 584 p. (In Russ.)
4. Sobol' I. M. *Monte-Karlo Numerical Methods*. M.: Nauka; 1973. 312 p. (In Russ.)
5. Blokhin A. V. *The Theory of Experiment*. Part 1. Minsk: Ehlektronnaya kniga BGU; 2002. 69 p. (In Russ.)

6. Budylin S. L. Judicial Activism or the Balance of Probabilities. The Russian and International Standards of Proof. *The Russian Federation Higher Arbitrazh Court Proceedings*. 2014;3:25–57. (In Russ.)
7. Kovalev F. V. *The Golden Ratio in Painting*. Kiev: Vyshcha shkola; 1989. 143 p. (In Russ.)
8. Korn G., Korn T. *Mathematics Handbook for Engineers and Researchers*. M.: Nauka; 1984. 832 p. (In Russ.)
9. Zimin M. M. The Application of Complex Functions to the Structural Risk Minimization Method. *Natural and Technical Sciences*. 2019;6:234–237. (In Russ.)
10. *Data Fitting Algorithms and Codes* / Ed. V. N. Vapnik. M.: Nauka; 1984. 816 p. (In Russ.)
11. Vapnik V. *Estimation of Dependences Based on Empirical Data*. New York: Springer-Verlag New York; 2006. 505 p.